



# Low temperature energy storage by bio-originated calcium alginate-octyl laurate microcapsules

Eszter Hajba-Horváth<sup>1</sup> · Bence Németh<sup>2</sup> · László Trif<sup>2</sup> · Zoltán May<sup>2</sup> · Miklós Jakab<sup>3</sup> · Andrea Fodor-Kardos<sup>2</sup> · Tivadar Feczko<sup>2</sup>

Received: 9 February 2022 / Accepted: 29 September 2022 / Published online: 21 October 2022  
© The Author(s) 2022

## Abstract

Octyl laurate phase change material (PCM) was microencapsulated by calcium alginate for eco-friendly low temperature energy storage. The PCM microcapsules were prepared by repeated interfacial coacervation followed by crosslinking method. In order to enhance the antibacterial properties of the as prepared capsules, the calcium alginate shell was functionalized by Ag nanoparticles. Calcium alginate-octyl laurate microcapsules possessed high latent heat of fusion values (130.8 and 128.6 J g<sup>-1</sup> on melting and cooling, respectively) which did not significantly change when Ag nanoparticles were entrapped in the shell (127.5 and 125.2 J g<sup>-1</sup> for melting and freezing enthalpy changes). Based on these values 71.0 and 69.0% maximal PCM content in the microcapsules were determined by the differential scanning calorimetry method. Both of the Ag-loaded and unloaded calcium alginate-octyl laurate PCM capsules maintained the high heat storing capacity after 250 warming and cooling cycles, which proved they did not suffer from leakage after the accelerated thermal test.

**Keywords** Phase change material · Low temperature energy storage · Biodegradable microcapsules

## Introduction

Energy storage is important to enhance energy savings especially when the world is struggling with the increasing concentration of greenhouse gases and consequently with climate change. Development of new technologies is necessary to reduce the use of fossil fuels and improve the energy efficiency [1]. Growing population and changing lifestyle have accompanied with increasing consumption of fresh and processed fruits and vegetables, meats, fish, dairy products and prepared foods [2]. For many high-value food products, the cold chain protection is required to preserve food quality. The microbial and chemical damages in food products can be delayed below 8 °C. Temperature fluctuation during food transportation influences its quality substantially. The lack of thermal insulation and thermal buffering capacity of packaged foods is a reason for shortening their shelf life. Packaging plays an essential role to protect food products from external impacts, such as microbiological, physiological, biochemical, organoleptic and physical deterioration [3]. Packaging might control ambient temperature variation. Common packaging materials have limited thermal buffering capacities. Paper, plastic, glass, metal and cardboard primarily used

✉ Tivadar Feczko  
tivadar.feczko@gmail.com

Eszter Hajba-Horváth  
hajba-horvath@mukki.richem.hu

Bence Németh  
nemeth.bence@mukki.richem.hu

László Trif  
trif.laszlo@ttk.mta.hu

Zoltán May  
may.zoltan@ttk.hu

Miklós Jakab  
jakab.miklos@mk.uni-pannon.hu

Andrea Fodor-Kardos  
kardos@mukki.richem.hu

<sup>1</sup> Research Institute of Biomolecular and Chemical Engineering, University of Pannonia, Egyetem u. 10, 8200 Veszprém, Hungary

<sup>2</sup> Institute of Materials and Environmental Chemistry, Research Centre for Natural Sciences, Magyar tudósok körútja 2., 1117 Budapest, Hungary

<sup>3</sup> Department of Materials Sciences and Engineering, Research Centre of Engineering Sciences, University of Pannonia, 8200 Veszprém, Hungary

in traditional commercial packages cannot impede temperature fluctuations [4]. Extensive research is needed in order to develop materials which are needed to reduce food waste owing to extended shelf life.

The three ways of storing energy are thermochemical energy storage, sensible and latent heat storage [5]. Latent heat storage occurs via heat absorption or release by the so-called phase change materials (PCMs) during a phase transition process such as melting (solid to liquid transition) and crystallization (liquid to solid transformation). Their main benefit is the high heat of fusion at a nearly constant temperature. Solid–liquid PCMs are capable of storing and releasing large amounts of heat within a narrow temperature range [6]. The PCMs can be classified as inorganic and organic compounds, and their eutectics. PCMs have been widely used in solar thermal energy storage [7], central air-conditioning systems [8], energy-efficient buildings [9], industrial waste heat recovery [10] and thermoregulating fibers [11]. Energy storage systems contribute to the growing demand of cooling in a sustainable way [12]. The low temperature thermal energy storage systems are mostly applied in air-conditioning [13] and thermal comfort [14], food [15] and medical cold chain logistics [16] and cold energy recovery from cryogenic energy storage [17]. Among cold storage strategies, PCMs have got very important role because of high energy storage density and nearly isothermal phase transition.

Organic PCMs may have benefits, such as high latent heat, low supercooling and vapor pressure, non-toxicity, low corrosiveness and good thermal reliability [18]. Main organic PCMs include paraffins, fatty alcohols, fatty acids [5] and fatty acid esters.

One of the most important difficulties of PCM use is liquid leakage in their molten state. Microencapsulation by form-stabilizing or into core–shell capsules can overcome this problem; moreover, it can increase the heat transfer by enhanced specific surface area against the bulk phase.

The global environmental problems regarding slowly or non-degradable plastic materials highlighted the need of new solutions also in the food packaging industry [4]. Beside food losses persistent plastic accumulation should be evaded by substituting these materials with fully biodegradable ones as was supported in the European Commission by a European Circular Economy Package, EU waste law [19]. The use of biomass-derived materials and biodegradable polymers as encapsulating components adds significant value to a product via the environmental advantages. In this respect, e.g., polycaprolactone and polylactide were used previously to encapsulate dodecane PCM by electrospinning technique with the aim of developing coating materials for low temperature energy storage [20]. Hoang et al. 2015 tested various biopolymers using also electrospinning and selected polycaprolactone as the most suitable shell material, since this material was capable of

encapsulating the largest amounts of PCM among the investigated polymers [3].

In our previous studies, paraffin [21] and coconut oil [22] PCMs were microencapsulated by Ca alginate shell with high heat storing capacity for use in building applications. Recently, the eco-friendly and biodegradable Ca alginate-coconut oil microparticles were functionalized by Ag nanoparticles in order to avoid too quick microbial degradation and increase the PCM microcapsule lifetime [23].

Octyl laurate and other fatty acid esters can be useful PCMs for low temperature energy storage with their high energy storage density, low volume change, cheap price, low vapor pressure and no toxicity [24]. Phase change temperature of octyl laurate (ca. 6–8 °C) suits the temperature requirement of cold chain logistics of medicines and foods.

The aim of the present paper is to study whether the microencapsulation method developed for paraffin and applied also for a fatty acid is suitable to encapsulate a fatty acid ester with low melting temperature in order to potentially use it in medical refrigeration transport system and cold-storage air-conditioning system at 2–8 °C. In order to enhance the lifetime of microcapsules, Ag nanoparticles were incorporated into the Ca alginate shell. During the formation of PCM microcapsules, the influence of the preparation conditions on the composition was examined. Finally, the core–shell morphology, PCM content, thermal properties as well as thermal reliability were investigated.

## Materials and methods

### Materials

Sodium alginate (viscosity at 25 °C, concentration 2 w/v%: 950 mPas) was bought from Cargill (Wayzata, Minnesota).  $\text{CaCl}_2 \cdot 2 \text{H}_2\text{O}$ ,  $\text{AgNO}_3$ , sodium citrate, sodium ascorbate and sodium nitrate were purchased from VWR International Kft. (Debrecen, Hungary). Petroleum ether (boiling temperature 60–62 °C) was purchased from Lach-Ner s.r.o (Nercetovice, Czech Republic). Polyvinyl alcohol (PVA, 87–90% hydrolyzed, MW  $\frac{1}{4}$  30,000–70,000) was purchased from Sigma Aldrich. Octyl laurate with the trade name of CrodaTherm™ 6.5 was a kind gift of Croda International Plc (Snaith, UK). All chemicals were of analytical grade and were used as purchased. For preparation of all aqueous solutions bi-distilled water was used.

### Preparation

#### Preparation of Ag nanoparticles

Sodium citrate,  $\text{AgNO}_3$  and sodium ascorbate solutions were used to prepare Ag nanoparticles according to the procedure shown in Table 1 and Fig. 1.

Solution “B” was added to solution “A” during continuous mixing at 1000 rpm by a Heidolph RZR 2051 control propeller stirrer. The duration of stirring was one hour. After this step the resulting dispersion was sedimented in a measuring cylinder overnight in order to separate the particles. The clear supernatant was slowly removed by a peristaltic pump (IKA PA-SF, IKA-Labortechnik, Staufen, Germany) paying attention to prevent resuspension. The sedimented particles were centrifuged by a Heraeus Biofuge primoR centrifuge at 8500 rpm at 25 °C for 30 min. After removing and discharging the supernatant, the particles were resuspended in approx. 5 mL distilled water and centrifuged by a Beckman Coulter Optima Max Ultracentrifuge at 20,000 rpm at 25 °C for 25 min. Then this washing step was repeated once. At the end of the procedure the particles were redispersed in distilled water resulting in approximately 6.5 mL suspension that was sonicated (Sonics VCX130, Sonics & Materials Inc., Newtown, CT) for 30 s at a power of 50%.

**Formation of calcium alginate-octyl laurate microcapsules**

For preparing the capsules the repeated interfacial coacervation/crosslinking method was applied that was previously developed by Németh et al. (2015) for coconut oil-loaded calcium alginate microparticles. Blank microcapsules (without Ag nanoparticles) and Ag-loaded calcium alginate-octyl laurate microcapsules were produced by this method (Fig. 2).

**Microcapsule preparation without Ag nanoparticles**

First of all, core particles were prepared by mixing 11–308 g 2% (m/m) sodium alginate aqueous solution and 4–112 g octyl laurate PCM and homogenizing them by a Sonics VCX130 sonicator (Sonics VCX130, Sonics & Materials Inc., Newtown, CT, US), IKA Ultra-Turrax (IKA-Werke, Staufen, Germany) or a Philips ProBlend 6 (900 W) smoothie machine at maximum speed for 2×2 min. 2 mL of the produced emulsion was pipetted dropwise into a 4% (m/m) CaCl<sub>2</sub> solution while stirring slowly by a magnetic stirrer (IKA-Labortechnik, Staufen, Germany). After the whole amount of the emulsion portion was pipetted, the solution containing the core particles was stirred further for 30 min. Then the particles were filtered and air-dried.

To coat the core particles with a calcium alginate shell, first they were placed in a 1.3% (m/m) sodium alginate solution for 10 min in order to completely immerse them in the liquid. Then the particles were carefully placed on a sieve to get rid of the excess alginate. After this step they were poured into 4% (m/m) CaCl<sub>2</sub> solution and stirred for 30 min using gentle magnetic stirring. The microcapsules were filtered, washed with distilled water, and then dried on a heated stainless steel plate at 120 °C for 15 min. The

**Table 1** Composition and volume of solutions used for Ag nanoparticle preparation

	Solution 1	Solution 2	Solution 3
Composition	0.2 M sodium citrate	0.2 M AgNO <sub>3</sub>	0.2 M sodium ascorbate
Volume (mL)	50	20	20
Solution A	Solution 1. + Solution 2. + 880 mL distilled water		
Solution B	Solution 3. + 30 mL distilled water		

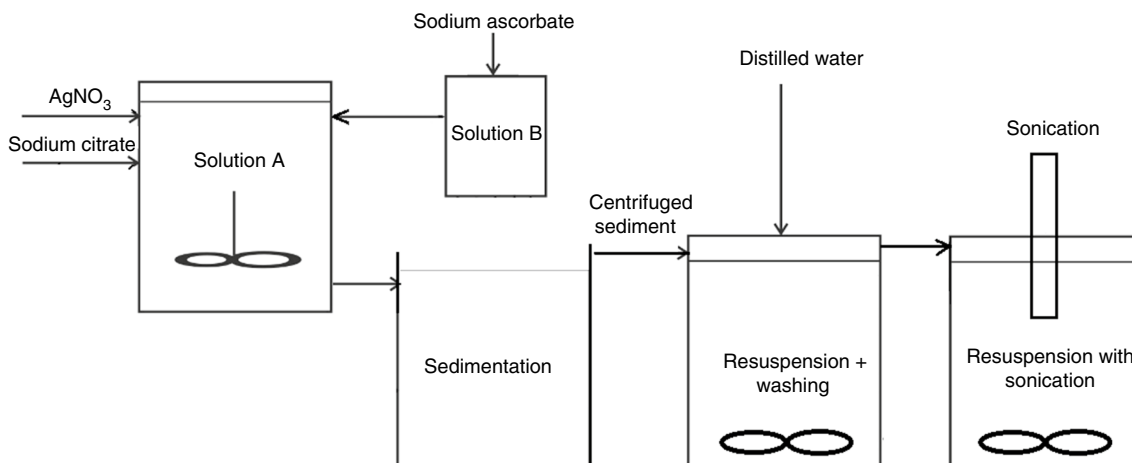


**Fig. 1** Scheme of Ag nanoparticle preparation

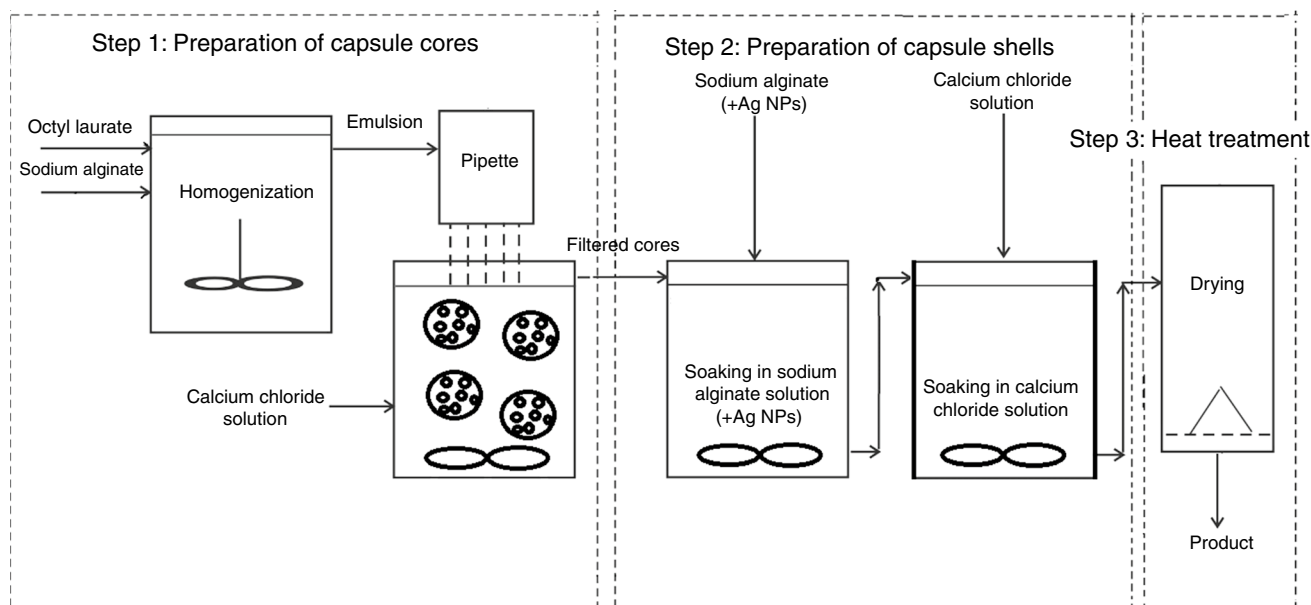


**Fig. 2** Scheme of calcium alginate-octyl laurate microcapsule preparation

uniform heat transfer to the wall of particles was resolved by their continuous movement.

### Ag-loaded microcapsule preparation

To prepare the Ag-functionalized calcium alginate-octyl laurate microcapsules the procedure discussed above was repeated except for the calcium alginate shell formation. After producing the core particles, 19.21 g 1.35% (m/m) sodium alginate aqueous solution was mixed with 0.74 mL Ag dispersion ( $35.2 \text{ mg mL}^{-1}$ ) and the mixture was sonicated (Sonics VCX130, Sonics & Materials Inc., Newtown, CT) for 30 s at a power of 60%. The prepared core particles were dropped into this solution and they went through the further steps detailed above until drying.

## Characterization

### Ag content determination of Ag dispersion

In order to determine the Ag content of the Ag dispersion prepared above, its 1 mL volume was centrifuged by a Hermle Z 216 MK centrifuge at 15,000 rpm at 25 °C for 30 min. The supernatant was removed and the dry mass of the pellet was determined after drying at 40 °C to constant mass.

### Size distribution of Ag nanoparticles

The size of Ag dispersion was studied by photon correlation spectroscopy method by means of Malvern Zetasizer ZS (Malvern Instruments, Malvern, UK) at 25 °C. 1 mL sample containing Ag dispersion and 1% PVA in 1:1 ratio was examined on five parallel samples.

### Determination of PCM content

For determination of octyl laurate content of the microcapsules 0.1 g of each type of microcapsules was weighed then ground with the help of a Narva microball mill (Narva DDR-GM9458, Brand-Erbisdorf, DDR). The PCM content of the ground capsules was dissolved using petroleum ether and vacuum filtered in order to separate the insoluble alginate. The organic solvent was evaporated at 50 °C in an oven. After evaporation, the remaining PCM was weighed. The PCM content of microcapsules was calculated by dividing the octyl laurate mass extracted from microcapsules by the total mass of the ground microcapsules.

### Microcapsule size and morphology

The size of the microcapsules (both blank and Ag-loaded capsules) was determined by an optical microscope (Carl Zeiss, Oberkochen, Germany). The diameter of 40 capsules

was measured based on the calibrated scale of the microscope, then the mean sizes and standard deviations were determined.

The morphology and cross section of microcapsules were imaged by a FEI Apreo scanning electron microscope (SEM, Thermofisher, USA) at 10 and 20 kV acceleration voltages. Microcapsules were placed on the specimen holder without any additional sample preparation. The shape of microcapsules did not change under vacuum ( $10^{-2}$  mbar).

### Determination of Ag content with ICP-OES

$3 \times 30$  mg microcapsules (three parallel measurements were done) were measured with analytical balance and put into glass beakers and 5 mL of concentrated nitric acid was poured to each parallel sample. The samples were heated and boiled until complete digestion (3–4 h heating). After cooling down, all samples were poured into 25 mL volumetric flasks and completed to 25 mL with MilliQ water (Suez,  $18.2 \text{ M}\Omega \text{ cm}^{-1}$ ) and measured with a Spectro Genesis ICP-OES instrument.

### DSC investigation

A Setaram  $\mu$ DSC3evo (Lyon, France) differential scanning calorimeter (DSC) was used to investigate the melting and freezing enthalpies before and after thermal cycling of the microcapsules. Weighed samples were loaded into the standard batch vessels of the microcalorimeter and were measured between 0 and 50 °C, with a scanning rate of 0.4 °C/min, then twice with a 0.2 °C/min scanning rate. The first cycle was set to vanish the thermal history of the samples, while the last cycle was a quality check of the second cycle. The obtained data were evaluated by the software (Calisto Processing, ver. 2.092, AKTS, Switzerland). The sensitivity was tested by a special calibration method (Joule effect), while the temperature range was calibrated with four certified reference materials (CRMs).

The microcapsules were heated and cooled in order to study their durability. The test was performed similarly to the literature [25] in a metal sample holder. The thermal cycling was done by a PC-controlled Peltier unit. 250 cycles were carried out by cooling the weighed microcapsules to -10, then heating them to 20 °C. DSC was performed after thermal cycling to examine whether the microcapsules leak the PCM in use.

### TG analysis

LabsysEvo (Setaram, Lyon, France) TG-DSC instrument was applied for thermogravimetric analysis using ( $90 \text{ mL min}^{-1}$ ) high purity (99.999%) synthetic air ( $20 \pm 1 \text{ v/v}\%$   $\text{O}_2$  in nitrogen) atmosphere. The heating range was 25 °C to

1000 °C with a heating speed of 10 °C/min. Before weighing them into the crucibles, a 100  $\mu\text{m}$  hole was drilled in the calcium alginate outer shell in order to avoid an explosive release of gases resulting from the evaporation of the PCM. The baseline correction and data processing was done by the software Calisto Processing, ver. 2.06. The multipoint calibration method was achieved to test the whole operating temperature range of instrument, while the microbalance was adjusted with two standard masses (50 and 500 mg, Sartorius GmbH, Germany, precision class E2) and the precision of the mass measurement was verified by the fifth molecule of water loss from a copper sulphate pentahydrate standard (Sigma-Aldrich, Spain).

## Results and discussion

### Physical and chemical characterization of microcapsules

Since it was verified in our previous study [23] that Ag nanoparticles dispersed in the shell of calcium alginate microcapsules exert efficient antibacterial and antifungal influence, they have been included in the shell of octyl laurate-loaded calcium alginate microparticles. The size of prepared Ag nanoparticles synthesized for the use in the microcapsule shell was investigated by photon correlation spectroscopy. Size distribution of prepared Ag nanoparticles (Fig. 3) with a mean size of  $130.0 \pm 1.6 \text{ nm}$  was very similar to that found in our previous study [23].

Octyl laurate-loaded calcium alginate microcapsules were prepared by repeated interfacial coacervation/crosslinking method. The fatty acid ester content of latent heat storing microcapsules was determined by a gravimetric method after extraction of PCM using petroleum ether in the first series of samples. 19 preliminary experiments without Ag nanoparticles and 4 ones with Ag nanoparticles

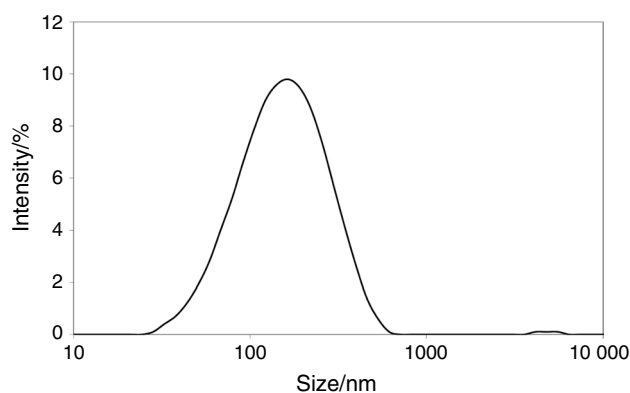
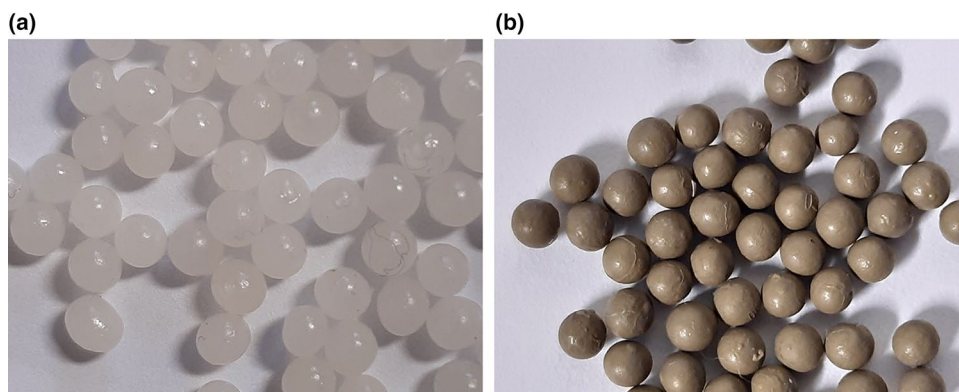


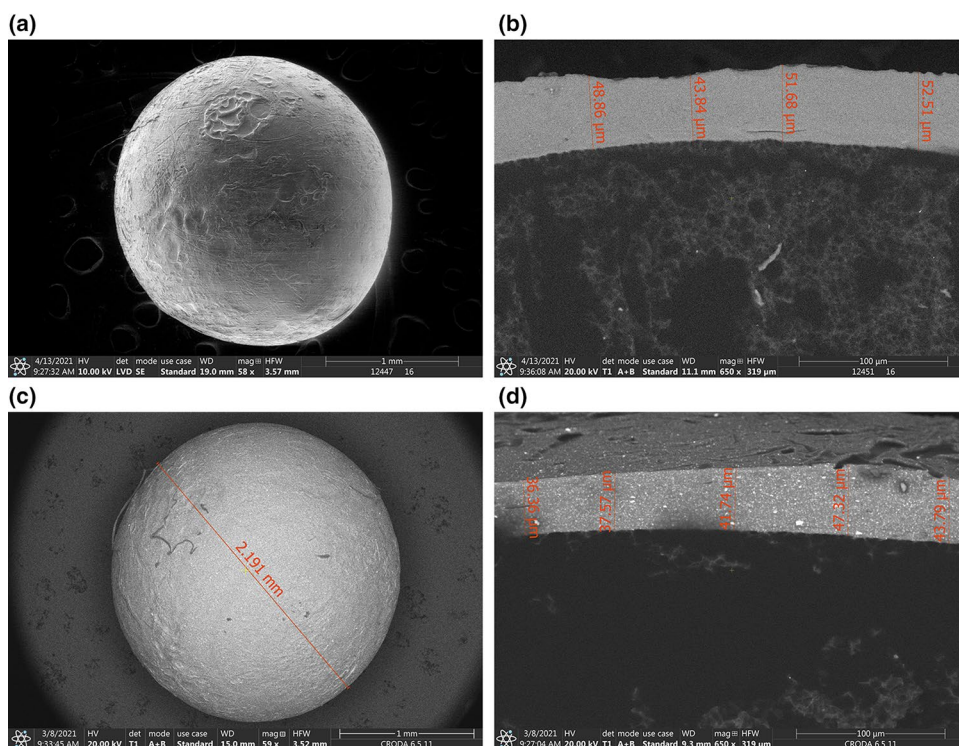
Fig. 3 Size distribution by intensity of Ag nanoparticles



**Fig. 4** Optical microscopic images of Ca alginate-octyl laurate microcapsules without (**a**, size:  $2.22 \pm 0.13$  mm) and with Ag nanoparticles (**b**, size:  $2.18 \pm 0.10$  mm)



**Fig. 5** SEM image of cetyl laurate-loaded calcium alginate microcapsules without (**a**, **b**) and with Ag nanoparticles in the shell (**c**, **d**)



showed that the homogenization process during the core formation has got of crucial importance considering the PCM content of microcapsules. Three different methods for homogenization were studied (see “[Microcapsule preparation without Ag nanoparticles](#)”), i.e., a sonicator, a high-shear mixer (Ultra-Turrax) and a smoothie machine. The quality of homogenization was reflected in the structure of microcapsule product. The homogenization was kept successful, when the capsule shell was continuous without any gap. Nevertheless, homogenization with a sonicator or a high-shear mixer resulted in deficient shell. The best homogenization was achieved by the Philips ProBlend 6 smoothie machine using the highest scale, providing continuous shell around the core; therefore, this

process was used for the samples prepared for further studies. PCM concentration in the formed microcapsules varied in the range of 47.5–63.0% m/m and 41.6–60.3% in calcium alginate-octyl laurate microcapsules without and with Ag, respectively.

Optical microscopy showed that both the Ag nanoparticle-loaded and unloaded calcium alginate-octyl laurate microcapsules had spherical shape and homogenous size distribution (Fig. 4).

Scanning electron microscopic measurements were performed for size and morphological analysis of the microcapsules (Fig. 5). The mean diameters of calcium alginate microcapsules were  $2.18 \pm 0.10$  and  $2.22 \pm 0.13$  mm in Ag-loaded and unloaded microcapsules; respectively,

(determined by optical microscopy) considering the size of 40 microcapsules/sample. The thickness of microcapsule shell was approximately 40–50  $\mu\text{m}$  (Fig. 5b and d). Homogeneously dispersed Ag nanoparticles can be observed as white dots in the cross section of microcapsule shell in Fig. 3d.

### DSC of PCM microcapsules

DSC analysis was performed to evaluate the heat capacity of PCM-loaded bio-originated microcapsules (Fig. 6). The octyl laurate PCM possessed  $181.8 \pm 0.2 \text{ J g}^{-1}$  melting and  $181.6 \pm 0.3 \text{ J g}^{-1}$  freezing enthalpy changes, while  $130.8 \pm 0.3 \text{ J g}^{-1}$  melting and  $128.6 \pm 0.4 \text{ J g}^{-1}$  freezing values were measured for calcium alginate-octyl laurate microcapsules. From these values, 71% m/m PCM content can be calculated in the microcapsules, which is similar to that we found previously in calcium alginate-coconut oil microcapsules [22]. However, due to the much higher melting and freezing enthalpy changes of octyl laurate, the latent heat storing capacity of the newly developed cooling microcapsules became more than 40% higher compared to the coconut oil-loaded microparticles. Ag nanoparticles involvement in the shell did not exert substantial influence on the heat storing capability of calcium alginate-octyl laurate microcapsules, since  $127.5 \pm 0.4$  and  $125.2 \pm 0.5 \text{ J g}^{-1}$  values were obtained for melting and freezing enthalpy changes, respectively. This corresponded to our expectations, since the Ag content of microcapsules was  $0.78 \pm 0.10\%$  m/m related to the total capsule mass measured by ICP-OES.

To hypothesize that an eco-friendly cooling box must be reusable, the developed calcium alginate-octyl laurate microcapsules must resist numerous cycles of heating and cooling without any damage during their lifetime. Thus, 250 melting–freezing cycles were applied on the microcapsules. After thermal cycling, the heat storing capability was studied by DSC to show any eventual change in the capacity of its phase change enthalpy. Figure 6 shows that the thermal cycling test did not result in leakage of PCM, hence the shell is resistant to the volume change during melting and freezing.

The Ag concentration of PCM particles was analyzed by ICP-OES. The Ag content of shell was lower than in the alginate solution, in which it was dissolved (Table 1). Since during the core formation the emulsion was composed of PCM and sodium alginate solution without Ag, this alginate increased the calcium alginate concentration of shell, while the Ag ratio was reduced.

### Thermal stability

In Fig. 7, the mass losses (TG) of the investigated samples are plotted against temperature.

It can be seen, that up to 180  $^{\circ}\text{C}$  all samples are losing a small mass (3–5%), which is due to the evaporation of the physically bound water. In the case of the shell constitutive material, calcium alginate, this mass loss is considerably higher, because the alginate structure binds quite high amount of water. On the mass loss curve of the PCM, between 180 and 365  $^{\circ}\text{C}$  there is a very large mass loss (which is accompanied by a large and sharp exothermic peak on the heat flow curve—not shown here), which corresponds to the evaporation and burning of the hydrocarbon content, in this step, 95% of the sample's mass is lost. In the case of the two capsules, a very similar high mass loss is noticeable in the above mentioned temperature range; however, their mass loss is between 78 and 80%. The calcium alginate shows a considerably smaller mass loss in this region (20.5%), due to the partial oxidative degradation of the alginate structure. In the next mass loss step (between 365 and 555  $^{\circ}\text{C}$ ), burn-out of the remaining organic content takes place in the case of all samples, however, the small mass loss (approximately 2.5%) in the case of the PCM material is surprising. A tentative explanation of this event could be that during the burning of the PCM, inside the crucible below the flame, under pyrolytic environment some carbonization takes place, which results in thermally more stable polymerized residue of higher molecular mass, which oxidizes at higher temperatures. The decomposition of the formed calcium carbonate originating from the burning of calcium alginate takes place in the 555–750  $^{\circ}\text{C}$  temperature region. The mass loss was 2.5% in the case of both capsules, and ~4% for the calcium alginate.

A tentative determination of the PCM content from the corresponding mass loss steps was also attempted. The basis of the calculation was the comparison (proportioning) of the mass losses of the PCM and the two capsules in the temperature region of the highest mass loss (180 and 365  $^{\circ}\text{C}$ ), and correcting the obtained PCM content by the small mass loss resulting from the burning of the calcium alginate shell. In the case of the two capsule samples, the amount of mass lost in this temperature region was calculated from the solid CaO residue resulting from their thermal degradation and from the decomposition of calcium alginate. The as determined PCM content for the two capsule samples are 75.5% m/m (calcium alginate-octyl laurate) and 76.7% m/m (calcium alginate-octyl laurate-Ag), which are in acceptable/good agreement with the PCM content determined by the microcalorimetric method. It should be also mentioned that the results of the above described calculations are significantly influenced by the calcium content of the capsule shell (in form of calcium alginate), which can vary from batch-to-batch preparation, thus altering the mass loss correction factor for this temperature range.

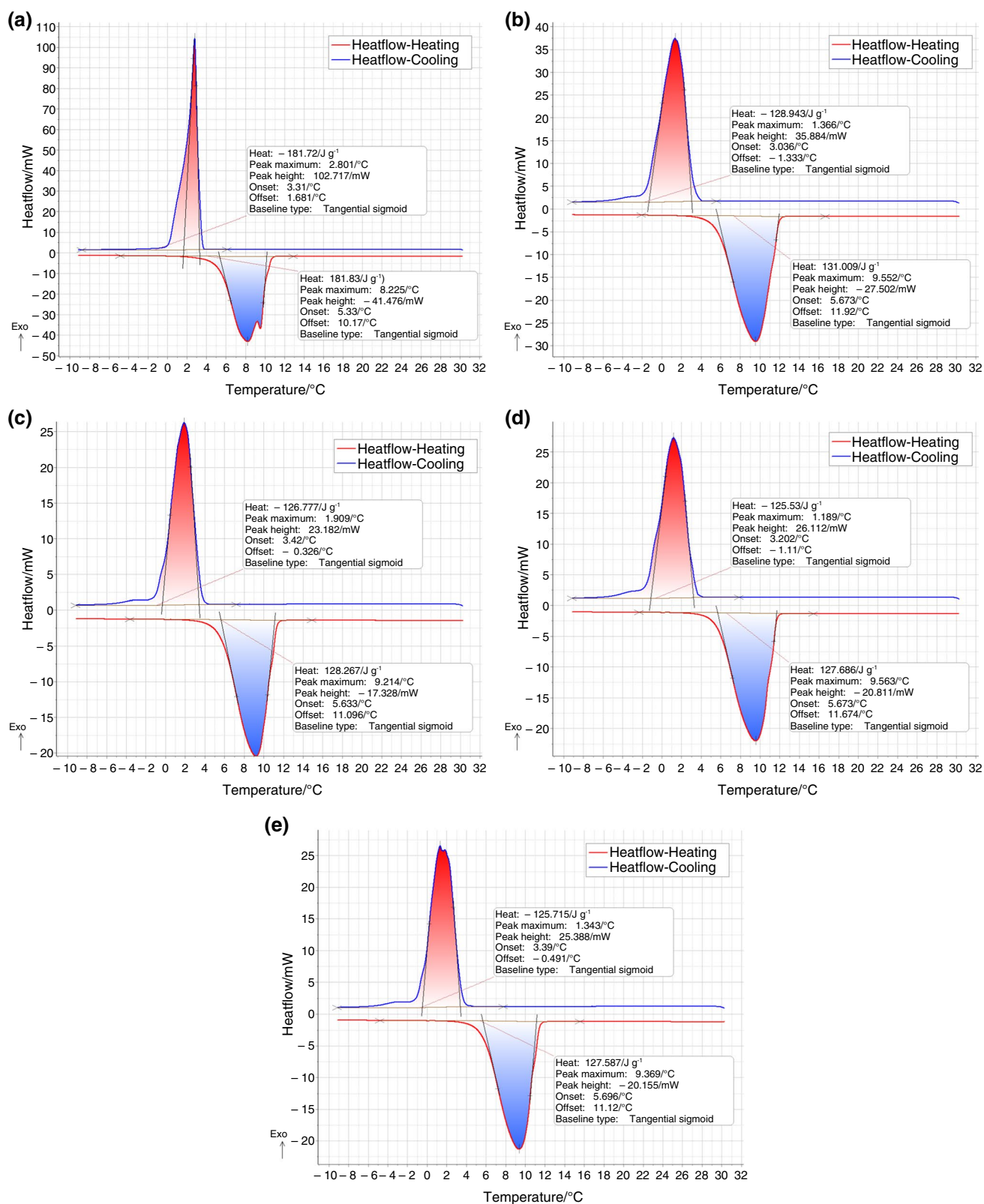


**Fig. 6** DSC of octyl laurate (a), PCM-loaded calcium alginate microcapsules before (b) and after thermal cycling (c) and Ag-loaded calcium alginate-octyl laurate microcapsules before (d) and after thermal cycling (e)



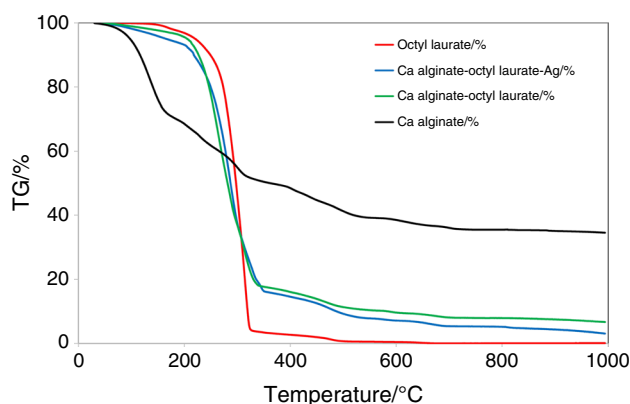


**Fig. 7** Mass loss (TG) curves of octyl laurate, calcium alginate and Ag-loaded as well as unloaded calcium alginate-octyl laurate microcapsules

## Conclusions

Fully bio-originated calcium alginate-octyl laurate microcapsules were formed for cold energy storage. The previously developed repeated interfacial coacervation method was improved to microencapsulate an organic material differing in hydrophobicity from the ones that have already been efficiently entrapped. Ag nanoparticles were loaded in the shell of microcapsules to add antimicrobial function. Calcium alginate-octyl laurate microcapsules had extremely high heat capacity which did not significantly reduce by Ag addition. 71.0% and 69.0% maximal PCM concentrations were reached in the microcapsules without or with Ag, respectively. Similarly high PCM content was also calculated from the TG results. The latent heat of fusion of fatty acid ester containing calcium alginate microcapsules did not decrease after 250 warming and cooling cycles, which denotes the microcapsules might be durably used in a bio-degradable food packaging.

**Acknowledgements** This work was supported by the grants provided by VEKOP-2.3.2-16-2017-00013 and 2020-1.1.2-PIACI-KFI-2021-00287 projects awarded by Ministry for Innovation and Technology. S/TEM studies were performed at the electron microscopy laboratory of the University of Pannonia, established using grant no. GINOP-2.3.3-15-2016-0009 from the European Structural and Investments Funds and the Hungarian Government.

**Author contributions** EHH and TF: Writing- Original Draft, Review & Editing. EHH, BN, LT, ZM and MJ: Investigation. AFK and TF Conceptualization. TF Project administration, Supervision.

**Funding** Open access funding provided by ELKH Research Centre for Natural Sciences.

## Declarations

**Conflict of interest** The authors declare that they have no conflict of interest.

**Open Access** This article is licensed under a Creative Commons Attribution 4.0 International License, which permits use, sharing, adaptation, distribution and reproduction in any medium or format, as long as you give appropriate credit to the original author(s) and the source, provide a link to the Creative Commons licence, and indicate if changes were made. The images or other third party material in this article are included in the article's Creative Commons licence, unless indicated otherwise in a credit line to the material. If material is not included in the article's Creative Commons licence and your intended use is not permitted by statutory regulation or exceeds the permitted use, you will need to obtain permission directly from the copyright holder. To view a copy of this licence, visit <http://creativecommons.org/licenses/by/4.0/>.

## References

- Du K, Calautit J, Wang ZH, Wu YP, Liu H. A review of the applications of phase change materials in cooling, heating and power generation in different temperature ranges. *Appl Energy*. 2018;220:242–73. <https://doi.org/10.1016/j.apenergy.2018.03.005>.
- Singh S, Gaikwad KK, Lee YS. Phase change materials for advanced cooling packaging. *Environ Chem Lett*. 2018;16(3):845–59. <https://doi.org/10.1007/s10311-018-0726-7>.
- Hoang HM, Leducq D, Perez-Masia R, Lagaron JM, Gogou E, Taoukis P, et al. Heat transfer study of submicro-encapsulated PCM plate for food packaging application. *Int J Refrig*. 2015;52:151–60. <https://doi.org/10.1016/j.ijrefrig.2014.07.002>.
- Madhan S, Espirito Santo C, Andrade LP, Silva PD, Gaspar PD. Active and intelligent packaging with phase change materials to promote the shelf life extension of food products. *KnE Eng*. 2020;5(6):232–41. <https://doi.org/10.18502/keg.v5i6.7037>.
- Sharma A, Shukla A, Chen CR, Wu T-N. Development of phase change materials (PCMs) for low temperature energy storage applications. *Sustain Energy Technol Assess*. 2014;7:17–21. <https://doi.org/10.1016/j.seta.2014.02.009>.
- Ghadim HB, Shahbaz K, Al-Shannaq R, Farid MM. Binary mixtures of fatty alcohols and fatty acid esters as novel solid-liquid phase change materials. *Int J Energy Res*. 2019;43(14):8536–47. <https://doi.org/10.1002/er.4852>.
- Pirdavari P, Hossainpour S. Numerical study of a Phase Change Material (PCM) embedded solar thermal energy operated cool store: a feasibility study. *Int J Refrig*. 2020;117:114–23. <https://doi.org/10.1016/j.ijrefrig.2020.04.028>.
- Porto TN, Delgado JMPQ, Guimaraes AS, Magalhaes HLF, Moreira G, Correia BB, et al. Phase change material melting process in a thermal energy storage system for applications in buildings. *Energies*. 2020;13(12):3254. <https://doi.org/10.3390/en13123254>.
- Rao VV, Parameshwaran R, Ram VV. PCM-mortar based construction materials for energy efficient buildings: a review on research trends. *Energy Build*. 2018;158:95–122. <https://doi.org/10.1016/j.enbuild.2017.09.098>.
- Li DC, Wang JH, Ding YL, Yao H, Huang Y. Dynamic thermal management for industrial waste heat recovery based on phase change material thermal storage. *Appl Energy*. 2019;236:1168–82. <https://doi.org/10.1016/j.apenergy.2018.12.040>.
- Haghighat F, Ravandi SAH, Esfahany MN, Valipouri A, Zarezade Z. Thermal performance of electrospun core-shell phase change fibrous layers at simulated body conditions. *Appl Therm Eng*. 2019;161:113924. <https://doi.org/10.1016/j.applthermaleng.2019.113924>.
- Wan X, Chen C, Tian SY, Guo BH. Thermal characterization of net-like and form-stable ML/SiO<sub>2</sub> composite as novel PCM for

- cold energy storage. *J Energy Storage*. 2020;28:101276. <https://doi.org/10.1016/j.est.2020.101276>.
13. Rakkappan SR, Sivan S, Ahmed SN, Naarendharan M, Sudhir PS. Preparation, characterisation and energy storage performance study on 1-Decanol-Expanded graphite composite PCM for air-conditioning cold storage system. *Int J Refrig*. 2021;123:91–101. <https://doi.org/10.1016/j.ijrefrig.2020.11.004>.
  14. Dhumane R, Mallow A, Qiao YY, Gluesenkamp KR, Graham S, Ling JZ, et al. Enhancing the thermosiphon-driven discharge of a latent heat thermal storage system used in a personal cooling device. *Int J Refrig*. 2018;88:599–613. <https://doi.org/10.1016/j.ijrefrig.2018.02.005>.
  15. Kong Q, Mu HL, Han YC, Wu WJ, Tong C, Fang XJ, et al. Biodegradable phase change materials with high latent heat: preparation and application on *Lentinus edodes* storage. *Food Chem*. 2021;364:130391. <https://doi.org/10.1016/j.foodchem.2021.130391>.
  16. Wu T, Xie N, Niu JY, Luo JM, Gao XN, Fang YT, et al. Preparation of a low-temperature nanofluid phase change material: MgCl<sub>2</sub>-H<sub>2</sub>O eutectic salt solution system with multi-walled carbon nanotubes (MWCNTs). *Int J Refrig*. 2020;113:136–44. <https://doi.org/10.1016/j.ijrefrig.2020.02.008>.
  17. Tafone A, Borri E, Cabeza LF, Romagnoli A. Innovative cryogenic Phase Change Material (PCM) based cold thermal energy storage for Liquid Air Energy Storage (LAES) - Numerical dynamic modelling and experimental study of a packed bed unit. *Appl Energ*. 2021;301:117417. <https://doi.org/10.1016/j.apenergy.2021.117417>.
  18. Li YY, Zhang XL, Munyalo JM, Tian Z, Ji J. Preparation and thermophysical properties of low temperature composite phase change material octanoic-lauric acid/expanded graphite. *J Mol Liq*. 2019;277:577–83. <https://doi.org/10.1016/j.molliq.2018.12.111>.
  19. Guillard V, Gaucel S, Fornaciari C, Angellier-Coussy H, Buche P, Gontard N. The next generation of sustainable food packaging to preserve our environment in a circular economy context. *Front Nutr*. 2018;5:121. <https://doi.org/10.3389/fnut.2018.00121>.
  20. Perez-Masia R, Lopez-Rubio A, Fabra MJ, Lagaron JM. Biodegradable polyester-based heat management materials of interest in refrigeration and smart packaging coatings. *J Appl Polym Sci*. 2013;130(5):3251–62. <https://doi.org/10.1002/app.39555>.
  21. Nemeth B, Nemeth AS, Toth J, Fodor-Kardos A, Gyenis J, Feczko T. Consolidated microcapsules with double alginate shell containing paraffin for latent heat storage. *Sol Energ Mater Sol Cells*. 2015;143:397–405. <https://doi.org/10.1016/j.solmat.2015.07.029>.
  22. Nemeth B, Nemeth AS, Ujhidy A, Toth J, Trif L, Gyenis J, et al. Fully bio-originated latent heat storing calcium alginate microcapsules with high coconut oil loading. *Sol Energy*. 2018;170:314–22. <https://doi.org/10.1016/j.solener.2018.05.066>.
  23. Nemeth B, Nemeth AS, Ujhidy A, Toth J, Trif L, Jankovics H, et al. Antimicrobial functionalization of Ca alginate-coconut oil latent heat storing microcapsules by Ag nanoparticles. *Int J Energy Res*. 2020;44(14):11998–2014. <https://doi.org/10.1002/er.5848>.
  24. Liston LC, Farnam Y, Krafcik M, Weiss J, Erk K, Tao BY. Binary mixtures of fatty acid methyl esters as phase change materials for low temperature applications. *Appl Therm Eng*. 2016;96:501–7. <https://doi.org/10.1016/j.applthermaleng.2015.11.007>.
  25. Sari A, Karaipekli A. Preparation, thermal properties and thermal reliability of capric acid/expanded perlite composite for thermal energy storage. *Mater Chem Phys*. 2008;109(2–3):459–64. <https://doi.org/10.1016/j.matchemphys.2007.12.016>.

**Publisher's Note** Springer Nature remains neutral with regard to jurisdictional claims in published maps and institutional affiliations.